

See discussions, stats, and author profiles for this publication at: <https://www.researchgate.net/publication/258244301>

Study of Ethanol Electrooxidation in Alkaline Electrolytes with Isotope Labels and Sum-Frequency Generation

ARTICLE *in* JOURNAL OF PHYSICAL CHEMISTRY LETTERS · SEPTEMBER 2011

Impact Factor: 7.46 · DOI: 10.1021/jz200957e

CITATIONS

21

READS

57

5 AUTHORS, INCLUDING:



Björn Braunschweig

Friedrich-Alexander-University of Erlangen-N...

39 PUBLICATIONS 446 CITATIONS

SEE PROFILE



Prabuddha Mukherjee

University of Illinois, Urbana-Champaign

25 PUBLICATIONS 855 CITATIONS

SEE PROFILE



Dana D. Slott

University of Illinois, Urbana-Champaign

297 PUBLICATIONS 6,651 CITATIONS

SEE PROFILE

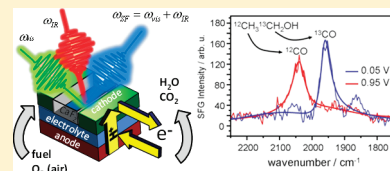
Study of Ethanol Electrooxidation in Alkaline Electrolytes with Isotope Labels and Sum-Frequency Generation

Robert B. Kutz, Björn Braunschweig, Prabuddha Mukherjee, Dana D. Dlott,* and Andrzej Wieckowski*

Department of Chemistry, University of Illinois at Urbana–Champaign, 600 South Mathews Avenue, Urbana, Illinois 61801, United States

Supporting Information

ABSTRACT: The ethanol electrooxidation reaction (EOR) on polycrystalline Pt catalysts in alkaline solution was studied for the first time with broadband sum-frequency generation (BB-SFG) spectroscopy. We find that C–C bond cleavage and CO formation occur as early as 0.05 V versus reversible hydrogen electrode (RHE), and that CO is oxidized at ~ 0.45 V, which is 0.2 V lower than in acidic media. In order to track the oxidation of single-carbon intermediates, we have monitored the oxidation of isotopically labeled ethanol ($^{12}\text{CH}_3^{13}\text{CH}_2\text{OH}$). Surface-adsorbed ^{12}CO and ^{13}CO are observed and show very different potential-dependent behaviors. ^{13}CO molecules formed from preoxidized carbon species such as $-\text{CH}_x\text{O}$, show the behavior expected from studies of CO-saturated alkaline media. ^{12}CO , however, which is indicative of the oxidation of methyl-like species ($-\text{CH}_x$) on the catalyst surface, is observed at unusually high potentials. The strongly adsorbed $-\text{CH}_x$ is not oxidatively removed from the surface until the electrode potential is swept past 0.65 V.

SECTION: Surfaces, Interfaces, Catalysis

Ethanol has become globally recognized as an important source of energy because it is abundant, has a high molecular energy density, and is easily produced from plant matter.¹ The majority of the ethanol produced in most industrial nations is used as a fuel additive for combustion engines as a means to reduce the dependency on foreign oil. However, using ethanol as a fuel in combustion engines is both inefficient and limited. Fuel blends with high ethanol content can pose public health risks,² and the thermodynamic losses inherent to combustion engines remain an issue. Ethanol fuel cells^{3–6} are ideally capable of bypassing these thermodynamic losses by converting chemical energy directly to electrical energy. Furthermore, both ethanol and fuel cells are clean and compactable, expanding the potential of ethanol fuel to power a wider variety of devices including portable electronics. Despite these advantages, the design of efficient ethanol fuel cell catalysts has proven to be highly challenging. It is clear from previous studies^{7–9} that the full potential of ethanol for fuel cells cannot be realized unless active catalyst surface sites for C–C bond splitting as well as CO and $-\text{CH}_x$ removal are simultaneously present and reaction conditions are optimized to promote higher selectivity toward CO_2 formation. For this reason, studies on the ethanol oxidation reaction (EOR) have been extensive,^{10–18} but they were primarily performed in acidic electrolytes. Alkaline electrolytes offer many advantages, however, particularly since electrocatalytic activity toward ethanol oxidation is much greater in alkaline than in acidic media.¹⁹ Furthermore, recent improvements on alkaline fuel cell designs include more robust membranes with reduced carbonation effects,²⁰ and improvements upon membranes resistant to carbonate precipitation bring them closer to performing as

efficiently as traditional proton exchange membranes.²¹ Thus, understanding and enhancing EOR catalysis in alkaline media is becoming increasingly pertinent.

For this reason, we have used broadband sum-frequency generation (BB-SFG) vibrational spectroscopy to study the EOR on a polycrystalline Pt surface in alkaline media. Polycrystalline Pt catalysts provide a good model system for studies of ethanol electrooxidation in alkaline media because they are widely known as highly active but inefficient catalysts for EOR.^{22,23} In order to establish the necessary characteristics of more efficient catalysts, we are interested in a molecular-level understanding of the EOR that reveals all possible steps that could decrease the overall efficiency. SFG, as an inherently surface-specific technique, provides a direct observation of only those molecular species that are adsorbed to the catalyst surface without spectral interference from the bulk electrolyte. The use of a Teflon spacer creates a fixed $25\ \mu\text{m}$ gap between the optical window and Pt electrode, permitting the synchronous application of voltammetric sweeps at rates of $<5\ \text{mV/s}$ without detrimental ohmic drop effects (for further details, see Supporting Information). Our data thus offer insights into the chemical identity of surface-adsorbed intermediates. We report new information on the mechanism of ethanol decomposition and CO formation in alkaline solution using isotopically labeled ethanol and clarify the behavior of adsorbed single-carbon

Received: July 13, 2011

Accepted: August 16, 2011

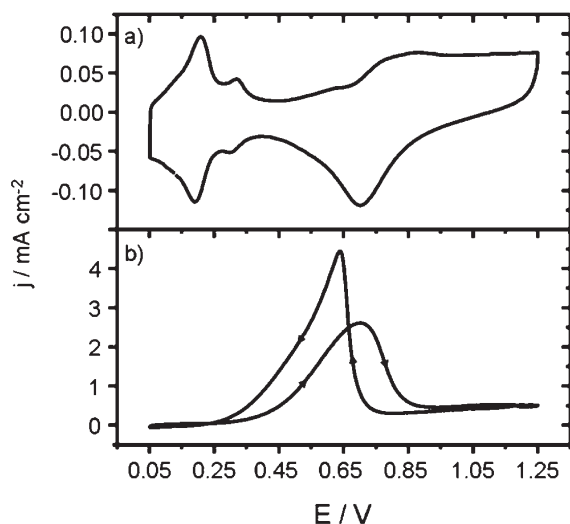


Figure 1. Hanging meniscus CVs of a polycrystalline Pt electrode in (a) blank 0.1 M NaOH and (b) 0.1 M NaOH with 0.5 M ethanol. The sweep rate for a and b was 50 mV/s.

intermediates that point to the presence of strongly adsorbed $-\text{CH}_x$ species in alkaline media.

Figure 1a,b presents cyclic voltammograms (CVs) of polycrystalline platinum in a solution of (a) blank 0.1 M NaOH and (b) 0.1 M NaOH with 0.5 M ethanol. These CVs were recorded in a hanging-meniscus configuration and with a sweep rate of 50 mV/s. The CV in Figure 1a shows features between 0.05 and 0.45 V that are characteristic for hydrogen underpotential deposition/desorption on a clean polycrystalline Pt surface. The formation of surface oxides on the anodic sweep starts at ~ 0.45 V, while on the cathodic sweep the reduction of the previously formed oxides gives rise to a negative feature centered at ~ 0.7 V. The CV in Figure 1b is characteristic of ethanol oxidation in alkaline media. The onset of the current feature centered between 0.4 and 0.85 V on the anodic potential sweep coincides with the oxidation of surface-adsorbed CO (Figure 2), which is preceded by the cleavage of ethanol's C–C bonds. The current density j decreases but remains above zero for the remainder of the anodic sweep, which implies some activity for oxidation of reaction intermediates at these potentials. The maximum in current density on the cathodic sweep is centered at ~ 0.6 V and coincides with the reductive stripping of Pt surface oxides.

In order to correlate the voltammetry with the formation and removal of specific intermediates of ethanol electrooxidation, consecutive SFG spectra were recorded in CO-saturated 0.1 M NaOH (Figure 2a) and in 0.1 M NaOH with 0.5 M ethanol (Figure 2b). In both solutions, a vibrational band centered at 2030 cm^{-1} dominates the SFG spectra and can be assigned to stretching vibrations of CO molecules adsorbed on Pt atop sites.²⁴ For potentials >0.35 V, the amplitude of the CO band for both CO-saturated and ethanol containing electrolytes (Figure 2) decreases with increasing surface oxide concentration (Figure 1a). However, a substantial recovery of the CO band at more anodic potentials between 0.75 and 1.25 V is observed in ethanol-containing solution (Figure 2b). We investigated this surprising potentiodynamic behavior of the CO intermediate in greater detail with a similar study using 0.5 M isotopically labeled ethanol ($^{12}\text{CH}_3\text{}^{13}\text{CH}_2\text{OH}$). Figure 2c presents the same spectral

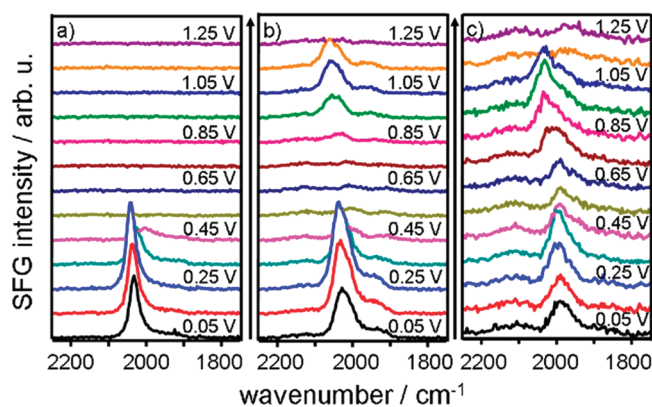


Figure 2. Potentiodynamic series of SFG spectra in 0.1 M NaOH with (a) CO-saturation, (b) 0.5 M ethanol ($\text{CH}_3\text{CH}_2\text{OH}$), and (c) 0.5 M isotopically labeled ethanol ($^{12}\text{CH}_3\text{}^{13}\text{CH}_2\text{OH}$). Potentials were as indicated in the figure. The acquisition time for each spectrum was 10 s for panel a, and 50 s for panels b and c. The broadband IR pulse was centered at 2030 cm^{-1} for panels a and b and 1990 cm^{-1} for panel c.

region for an experiment where isotopically labeled ethanol is oxidized. Consistent with previous experiments with regular ethanol, oxidation of isotopically labeled ethanol leads to an identical decrease and sudden increase of the CO band at higher potentials: At 0.05 V, a band at 1995 cm^{-1} attributable to ^{13}CO is observed, increases in intensity with increasing potential, and begins to diminish at 0.35 V. However, an apparent abrupt blue-shift of CO stretching frequencies to $\sim 2030\text{ cm}^{-1}$ takes place, while the SFG intensity near 1995 cm^{-1} rapidly diminishes (Figure 2c). It is very unlikely that potential-induced Stark tuning would be responsible for such an abrupt and dramatic frequency shift, as our further analysis demonstrates. Consequently, the band at 0.75 V must be composed of two bands at $\sim 2030\text{ cm}^{-1}$ and $\sim 1995\text{ cm}^{-1}$ that are attributable to ^{12}CO and ^{13}CO species, respectively. This conclusion is further substantiated by our SFG spectra at 0.85 V, where the ^{12}CO signal has clearly resolved into a band at 2030 cm^{-1} , and the ^{13}CO signal at 1995 cm^{-1} has fully diminished in amplitude (Figure 2c).

In order to obtain a better understanding of the potential dependence of the reported vibrational bands, we have fitted our vibrational spectra with model functions according to eq 1 (Supporting Information). The amplitudes A_q of CO atop from regular ethanol and CO atop from isotopically labeled ethanol are shown as a function of electrode potential in Figure 3a,b, respectively. Clearly, at low potentials in Figure 3b, there is no ^{12}CO vibrational band. Surface-bound ^{12}CO species that would give rise to the latter band are formed at potentials >0.75 V only. The frequencies ω_q of the ^{13}CO and ^{12}CO from the oxidation of 0.5 M regular ethanol and 0.5 M isotopically labeled ethanol are shown as a function of electrode potential in Figure 3c,d, respectively.

Spectra were also recorded in lower-concentration solutions of 0.2 M regular ethanol and isotopically labeled ethanol. We present these spectra as well because they more dramatically demonstrate the frequency separation between the ^{13}CO and ^{12}CO vibrational bands. A comparison of spectra modeled according to eq 1 is presented in Figure 4. Figure 4a shows CO vibrational bands from 0.2 M regular ethanol at 0.05 V and at 0.95 V. Similarly, Figure 4b shows CO vibrational bands from 0.2 M isotopically labeled ethanol at 0.05 V, where ^{13}CO dominates the

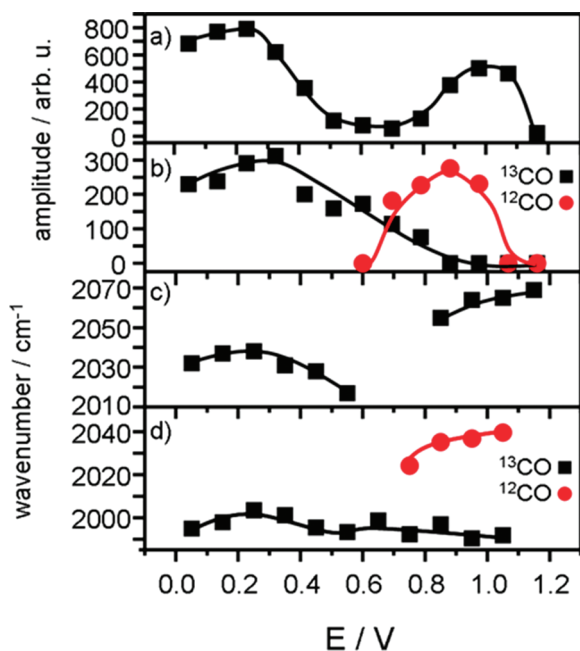


Figure 3. Potential dependence of SFG amplitudes for the vibrational bands in 0.1 M NaOH centered at (a) 2030 cm^{-1} with 0.5 M regular ethanol (Figure 2b) and (b) 2010 cm^{-1} and 1970 cm^{-1} with 0.5 M $^{12}\text{CH}_3\text{ }^{13}\text{CH}_2\text{OH}$ (Figure 2c). Frequencies of the CO vibrational bands from (c) 0.5 M regular ethanol (Figure 2b) and (d) 0.5 M $^{12}\text{CH}_3\text{ }^{13}\text{CH}_2\text{OH}$ (Figure 2c).

spectrum, and at 0.95 V, where ^{12}CO dominates the spectrum. The more pronounced frequency shift in isotopically labeled ethanol further emphasizes the hypothesis that these two vibrational bands are indicative of two different single-carbon species on the ethanol molecule.

Complete oxidation of ethanol to CO_2 requires both the splitting of the C–C bond and the subsequent oxidative removal of surface-adsorbed carbonaceous fragments. An ideal catalyst with a high selectivity for ethanol oxidation toward CO_2 formation, therefore, requires persistently available active sites that can catalyze both of these processes. Our observation of surface-adsorbed CO molecules at 0.05 V indicates that on a polycrystalline Pt surface, the ethanol molecule's C–C bond breaks at very low potentials and, subsequent to the dissociation of the ethanol molecule, at least one of the resulting single-carbon fragments can be further oxidized to CO. This scission of the C–C bond at low potentials is similarly observed in acidic media,¹⁶ but in alkaline media the resulting single-carbon fragments show remarkably different behavior. While in acidic solutions CO oxidation typically occurs at potentials of ~ 0.65 V,¹⁶ it is observed at much lower potentials of 0.25 to 0.35 V in alkaline electrolytes (Figure 2). Comparing the onsets for CO oxidation in acidic and alkaline electrolytes, we suggest that CO oxidation is more facile in alkaline than in acidic electrolytes as a result of a higher hydroxyl coverage at more cathodic potentials (Figure 1a). Moreover, the presence and the oxidation of CO as a product of ethanol electrooxidation is consistent with the expected behavior in CO-saturated alkaline and acidic solutions reported in this and previous studies.^{24,25} CO is, however, also observed at unusually high potentials, which are well inside the region of oxide formation on polycrystalline Pt electrodes in blank alkaline electrolytes. In order to address the possible origin

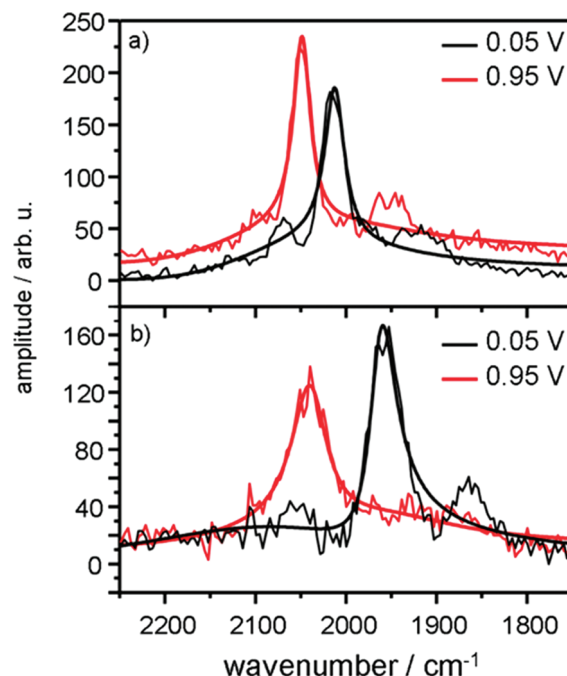


Figure 4. Comparison of the spectra for CO vibrational bands from solutions of (a) 0.2 M regular ethanol and (b) 0.2 M isotopically labeled ethanol ($^{12}\text{CH}_3\text{ }^{13}\text{CH}_2\text{OH}$) at potentials of 0.05 and 0.95 V. Modeled spectra are bolded and superimposed over their respective raw spectra to clearly indicate the position of each CO band.

of the CO recovery, which appears to belie the relative ease of oxidizing CO in alkaline media, we tracked the oxidation of the different carbon species that are immediate products of ethanol C–C bond cleavage. In particular, subsequent oxidation of the resulting $^{12}\text{CH}_x$ and $^{13}\text{COH}_x$ fragments from isotopically labeled ethanol ($^{12}\text{CH}_3\text{ }^{13}\text{CH}_2\text{OH}$) results in surface adsorbed ^{12}CO and ^{13}CO .

In previous work¹⁶ on ethanol oxidation in acidic media with isotopic labeling, we have demonstrated that oxidation of partially oxidized $-\text{CH}_x\text{O}$ fragments occurs more rapidly at lower overpotentials compared to $-\text{CH}_x$ fragments, which resist further oxidation and persist on the Pt surface as a catalyst poison. It is reasonable to assume the absence of catalytic sites for efficient oxidation of $-\text{CH}_x$ on polycrystalline Pt in alkaline electrolytes as well. This conclusion is corroborated by our SFG spectra during electrooxidation of $^{12}\text{CH}_3\text{ }^{13}\text{CH}_2\text{OH}$, where at low potentials the formation of ^{13}CO is observed only, while ^{12}CO bands that can be expected from $^{12}\text{CH}_x$ oxidation are absent. A complete change of the situation takes place at high anodic potentials where ^{13}CO is absent and ^{12}CO dominates the SFG spectra. A sudden shift at 0.75 V in SFG intensity from the lower-frequency ^{13}CO band to the higher-frequency ^{12}CO band, displayed in Figure 2c and further clarified in Figure 3d, unequivocally demonstrates the oxidative stripping of ^{13}CO from the Pt surface and the simultaneous deposition of ^{12}CO . Further proof that possible bulk oxidation of ethanol does not produce CO vibrational bands at these potentials can be found in the observation that on a reverse potential sweep to 0.05 V, no CO bands were observed in the potential range between 0.85 and 1.25 V (Figure S1, Supporting Information). Therefore, the observed CO band must originate from the oxidation of previously formed $-\text{CH}_x$. At these potentials, CO is quickly oxidized to CO_2 , and the

remaining free adsorption sites are then covered with surface oxides, which inhibit further oxidation reactions. At this point it should be noted that our results are in agreement with a voltammetric study by Lai and Koper,⁴ where the presence of stable $-\text{CH}_x$ intermediates on Pt(111) terrace sites in alkaline media is suggested. On polycrystalline Pt electrodes, there is an abundance of (111) surface sites, and, consequently, strongly adsorbed and stable $-\text{CH}_x$ species can exist on (111) sites of the polycrystalline Pt electrode as well. Bayer et al. also document a single-carbon species that can be reduced to methane at potentials below 0.2 V.²⁶ However, so far, direct and persuasive spectroscopic evidence of such a species in alkaline media has eluded the community.⁷ Furthermore, our results provide evidence that an anodic potential sweep to potentials of >0.65 V yields oxidation of $-\text{CH}_x$. Here, the supporting electrolyte may play a crucial role and act as a cocatalyst that lowers the overpotential for the latter reaction.

In acidic media, the $-\text{CH}_x$ intermediate is oxidized to ^{12}CO even at potentials as low as 0.05 V, albeit only in relatively very small quantities.^{16,27} We do not observe the same ^{12}CO peak at low potentials in alkaline media. This could be due to a much weaker intensity of the CO vibrational band in alkaline media. However, Severson et al. demonstrated that molecular dipole–dipole coupling between adsorbed ^{12}CO and ^{13}CO molecules dramatically shifts vibrational band intensity from the ^{13}CO to the ^{12}CO vibrational band.²⁸ Thus, if ^{12}CO is present on the surface at low potentials in alkaline media, it must be in very small quantities indeed for us to be unable to observe it. For high anodic potentials where ^{12}CO dominates the spectra, the possible presence of ^{13}CO cannot entirely be ruled out, but is extremely unlikely as we do not observe this band during the cathodic sweep.

In conclusion, we have presented the first BB-SFG study of ethanol electrooxidation in alkaline media that permits new insights into the behavior of single-carbon species as a result of carbon–carbon bond splitting on the Pt electrode. In addition to the low overpotential for CO oxidation at ~ 0.35 V, we observed a recovery of the CO vibrational band at unusually high anodic potentials of 0.75 to 1.15 V. This hitherto unexpected behavior was investigated in detail with isotopically labeled ethanol and points to the presence of strongly adsorbed single-carbon species such as $-\text{CH}_x$, which resist oxidation for potentials <0.75 V. Our results clearly demonstrate that the advantage of alkaline media—an oxidative removal of surface-bound CO at much lower overpotentials—is thus impaired by the persistence of strongly adsorbed $-\text{CH}_x$ species, which block adsorption sites for the ethanol fuel and lead to a decrease in overall efficiency. It is now quite clear that the surface composition of more efficient catalysts will require active surface sites for C–C bond breaking and CO removal as well as an increased selectivity for CO_2 formation. However, the highest efficiencies can be achieved only if these surface sites are accompanied by active sites that also remove strongly bound $-\text{CH}_x$ species from the surface.

■ ASSOCIATED CONTENT

S Supporting Information. Experimental details, a description of the modeling method, and an additional figure showing spectra recorded on a cathodic-going potential sweep. This material is available free of charge via the Internet at <http://pubs.acs.org>.

■ AUTHOR INFORMATION

Corresponding Author

*E-mail: dlott@scs.illinois.edu (D.D.D.); andrzej@scs.illinois.edu (A.W.).

■ ACKNOWLEDGMENT

Research described in this study was supported by the U.S. Army Research Office under Award W911NF-08-10309. D.D.D. acknowledges partial support from the U.S. Air Force Office of Scientific Research under Award FA9550-09-1-0163. B.B. gratefully acknowledges support by Professor Martin Gruebele and financial support from a Feodor Lynen fellowship of the Alexander von Humboldt Foundation.

■ REFERENCES

- (1) Lynd, L. R.; Cruz, C. H. D. B. Make Way for Ethanol. *Science* **2010**, *330*, 1176–1177.
- (2) Jacobson, M. Z. Effects of Ethanol(E85) versus Gasoline Vehicles on Cancer and Mortality in the United States. *Environ. Sci. Technol.* **2007**, *41*, 4150–4157.
- (3) Heinen, M.; Jusys, Z.; Behm, R. J. Ethanol, Acetaldehyde and Acetic Acid Adsorption/Electrooxidation on a Pt Thin Film Electrode under Continuous Electrolyte Flow: An in Situ ATR-FTIRS Flow Cell Study. *J. Phys. Chem. C* **2010**, *114*, 9850–9864.
- (4) Koper, M. T. M.; Lai, S. C. S. Ethanol Electro-oxidation on Platinum in Alkaline Media. *Phys. Chem. Chem. Phys.* **2009**, *11*, 10446–10456.
- (5) Giz, M. J.; Camara, G. A. The Ethanol Electrooxidation Reaction at Pt(111): The Effect of Ethanol Concentration. *J. Electroanal. Chem.* **2009**, *625*, 117–122.
- (6) Lai, S. C. S.; Koper, M. T. M. Electro-oxidation of Ethanol and Acetaldehyde on Platinum Single-Crystal Electrodes. *Faraday Discuss.* **2008**, *140*, 399–416.
- (7) Lai, S. C. S.; Kley, S. E. F.; Rosca, V.; Koper, M. T. M. Mechanism of the Dissociation and Electrooxidation of Ethanol and Acetaldehyde on Platinum As Studied by SERS. *J. Phys. Chem. C* **2008**, *112*, 19080–19087.
- (8) Gomes, J. F.; Busson, B.; Tadjeddine, A.; Tremiliosi-Filho, G. Ethanol Electro-oxidation over Pt(*h k l*): Comparative Study on the Reaction Intermediates Probed by FTIR and SFG Spectroscopies. *Electrochim. Acta* **2008**, *53*, 6899–6905.
- (9) Vigier, F.; Rousseau, S.; Coutanceau, C.; Leger, J. M.; Lamy, C. Electrocatalysis for the Direct Alcohol Fuel Cell. *Top. Catal.* **2006**, *40*, 111–121.
- (10) Camara, G. A.; Iwasita, T. Parallel Pathways of Ethanol Oxidation: The Effect of Ethanol Concentration. *J. Electroanal. Chem.* **2005**, *578*, 315–321.
- (11) de Souza, J. P. I.; Queiroz, S. L.; Bergamaski, K.; Gonzalez, E. R.; Nart, F. C. Electro-oxidation of Ethanol on Pt, Rh, and PtRh Electrodes. A Study Using DEMS and in-Situ FTIR Techniques. *J. Phys. Chem. B* **2002**, *106*, 9825–9830.
- (12) Tarnowski, D. J.; Korzeniewski, C. Effects of Surface Step Density on the Electrochemical Oxidation of Ethanol to Acetic Acid. *J. Phys. Chem. B* **1997**, *101*, 253–258.
- (13) Xia, X. H.; Liess, H.-D.; Iwasita, T. Early Stages in the Oxidation of Ethanol at Low Index Single Crystal Platinum Electrodes. *J. Electroanal. Chem.* **1997**, *437*, 233–240.
- (14) Lee, A. F.; Gawthrop, D. E.; Hart, N. J.; Wilson, K. A.; Fast, X. P. S. Study of the Surface Chemistry of Ethanol over Pt {111}. *Surf. Sci.* **2004**, *548*, 200–208.
- (15) Shao, M. H.; Adzic, R. R. Electrooxidation of Ethanol on a Pt Electrode in Acid Solutions: in Situ ATR-SEIRAS Study. *Electrochim. Acta* **2005**, *50*, 2415–2422.
- (16) Kutz, R. B.; Braunschweig, B.; Mukherjee, P.; Behrens, R. L.; Dlott, D. D.; Wieckowski, A. Reaction Pathways of Ethanol Electrooxidation

on Polycrystalline Platinum Catalysts in Acidic Electrolytes. *J. Catal.* **2010**, 278, 181–188.

(17) Xu, C. W.; Shen, P. K. Novel Pt/CeO₂/C Catalysts for Electrooxidation of Alcohols in Alkaline Media. *Chem. Commun.* **2004**, 2238–2239.

(18) Kwon, Y.; Lai, S. C. S.; Rodriguez, P.; Koper, M. T. M. Electrocatalytic Oxidation of Alcohols on Gold in Alkaline Media: Base or Gold Catalysis? *J. Am. Chem. Soc.* **2011**, 133, 6914–6917.

(19) Lai, S. C. S.; Kleijn, S. E. F.; Öztürk, F. T. Z.; van Rees Vellinga, V. C.; Koning, J.; Rodriguez, P.; Koper, M. T. M. Effects of Electrolyte pH and Composition on the Ethanol Electro-oxidation Reaction. *Catal. Today* **2010**, 154, 92–104.

(20) Varcoe, J. R.; Slade, R. C. T. An electron-Beam-Grafted ETFE Alkaline Anion-Exchange Membrane in Metal-Cation-Free Solid-State Alkaline Fuel Cells. *Electrochem. Commun.* **2006**, 8, 839–843.

(21) Lu, J. P. S.; Li, Y.; Huang, A.; Lu, L. Z. J. High-Performance Alkaline Polymer Electrolyte for Fuel Cell Applications. *Adv. Funct. Mater.* **2010**, 20, 312–319.

(22) Lamy, C.; Lima, A.; LeRhun, V.; Delime, F.; Coutanceau, C.; Léger, J.-M. Recent Advances in the Development of Direct Alcohol Fuel Cells (DAFC). *J. Power Sources* **2002**, 105, 283–296.

(23) Lamy, C.; Rousseau, S.; Belgsir, E. M.; Coutanceau, C.; Leger, J. M. Recent Progress in the Direct Ethanol Fuel Cell: Development of New Platinum–Tin Electrocatalysts. *Electrochim. Acta* **2004**, 49, 3901–3908.

(24) García, G.; Rodríguez, P.; Rosca, V.; Koper, M. T. M. Fourier Transform Infrared Spectroscopy Study of CO Electro-oxidation on Pt(111) in Alkaline Media. *Langmuir* **2009**, 25, 13661–13666.

(25) Lu, G. Q.; Lagutchev, A.; Dlott, D. D.; Wieckowski, A. Quantitative Vibrational Sum-Frequency Generation Spectroscopy of Thin Layer Electrochemistry: CO on a Pt Electrode. *Surf. Sci.* **2005**, 585, 3–16.

(26) Bayer, D.; Berenger, S.; Joos, M.; Cremers, C.; Tubke, J. Electrochemical Oxidation of C-2 Alcohols at Platinum Electrodes in Acidic and Alkaline Environment. *Int. J. Hydrogen Energ.* **2010**, 35, 12660–12667.

(27) Souza-Garcia, J.; Herrero, E.; Feliu, J. M. Breaking the C–C Bond in the Ethanol Oxidation Reaction on Platinum Electrodes: Effect of Steps and Ruthenium Adatoms. *ChemPhysChem* **2010**, 11, 1391–1394.

(28) Severson, M. W.; Stuhlmann, C.; Villegas, I.; Weaver, M. J. Dipole–Dipole Coupling Effects upon Infrared Spectroscopy of Compressed Electrochemical Adlayers: Application to the Pt(111)/CO System. *J. Chem. Phys.* **1995**, 103, 9832–9843.